

# Optical Binding Between Nanowires

Stephen H. Simpson<sup>a</sup> and Simon Hanna<sup>b</sup>

<sup>a</sup>Institute of Scientific Instruments of the ASCR, v.v.i., Královopolská 147, 612 64 Brno, Czech Republic

<sup>b</sup>H.H. Wills Physics Laboratory, University of Bristol, Tyndall Avenue, Bristol BS8 1TL, UK

## ABSTRACT

Optical binding occurs in systems of both dielectric and metal particles and results in the formation of clusters and coupled dynamical behaviour. Optical binding between spherical particles has been long studied, but comparatively little work has appeared describing binding in lower symmetry systems. In this paper we discuss recent theoretical work and computer simulations of optical binding between nanowires in linearly polarised counter propagating beams.

**Keywords:** Optical binding, counter-propagating plane waves, nanowires, computer simulation, coupled dipole method

## 1. INTRODUCTION

The phenomenon of optical binding was first observed over twenty-five years ago.<sup>1</sup> The optical binding effect results from the optical forces that arise between particles as a result of multiple scattering. Optical binding forces can result in a number of consequences including arranging matter into regular, crystalline arrays<sup>2</sup> and the production of complex, non-conservative, quasi-periodic motion.<sup>3</sup> Most studies of optical binding have been performed using moderately scattering dielectric spheres (e.g. silica),<sup>4-6</sup> although there have been some recent departures from this trend including ultra-strongly bound nanoparticles,<sup>7,8</sup> plasmonic silver bipyramids<sup>9</sup> and carbon nanotubes.<sup>10</sup> The reduction of particle symmetry introduces extra complexity. For example, torques can be applied to non-spherical objects by the external field, as well as by the scattered field from neighbouring particles. This may be expected to have consequences for the organizational properties of these systems.

In addition to fundamental considerations, there is increasing interest in practical techniques for organising nanostructures.<sup>11,12</sup> While optical tweezers have been successfully applied to the task of nanoparticle manipulation,<sup>13-17</sup> the application of optical binding has been focused, to a great extent, on the behaviour of spherical particles. Here we study the behaviour of dielectric nanowires held in linearly-polarised counter-propagating plane waves. From previous computer simulations we have shown that nanowires orient with the polarisation of such plane waves, and have the tendency to form ladder-like structures, with the rungs of the ladder separated by approximately the wavelength of light in the surrounding medium.<sup>18</sup> In the present paper, we consider the influence of the nanowire geometry (length and diameter) on the stability of the ladder-like bound states.

## 2. METHODS

### 2.1 Computational model

Optical binding experiments are often performed with particles immersed in a viscous medium, such as water. The subsequent motion of the bound particles is therefore determined by their hydrodynamic interactions, including stochastic, Brownian forces, as well as by any position-dependent optical forces. In the present computer model, we include all optical and hydrodynamic interactions, including fluctuations, using a coarse-grained approach. The nanowires are represented by rigid lines of small spheres, which act as the centres for both the hydrodynamic and optical calculations. Although, at the outset, this may appear to be a crude approximation, the basic scheme may be extended, arbitrarily, to improve the accuracy and realism of the results.

---

Further author information: (Send correspondence to S.H.)

S.H.: E-mail: [s.hanna@bristol.ac.uk](mailto:s.hanna@bristol.ac.uk), Telephone: +44 117 928 8771

The system consists of  $N_{ns}$  identical nano-wires, each comprising  $n_b$  beads, giving a total of  $N_b = n_b N_{ns}$  beads in the system. The force on the beads is given by a vector of length  $3N_b$ , consisting of a list of the force components on each bead in turn:

$$\mathbf{f} = \left( f_{1,x}^1, f_{1,y}^1, f_{1,z}^1, f_{1,x}^2, \dots, f_{1,z}^{n_b}, f_{2,x}^1, \dots, f_{2,z}^{n_b}, \dots, f_{N_{ns},z}^{n_b} \right). \quad (1)$$

Similarly, the bead velocities are given by:

$$\mathbf{v} = \left( v_{1,x}^1, v_{1,y}^1, v_{1,z}^1, v_{1,x}^2, \dots, v_{1,z}^{n_b}, v_{2,x}^1, \dots, v_{2,z}^{n_b}, \dots, v_{N_{ns},z}^{n_b} \right) \quad (2)$$

These quantities are re-expressed in terms of the rigid-body motions of the nanowires alone. These latter quantities are represented by vectors of length  $6N_s$ , for the forces (including torques) and velocities (including rotations):

$$\mathbf{F} = (\mathbf{F}_1, \mathbf{T}_1, \mathbf{F}_2, \mathbf{T}_2, \dots, \mathbf{F}_{N_{ns}}, \mathbf{T}_{N_{ns}}) = (F_{1,x}, F_{1,y}, F_{1,z}, T_{1,x}, T_{1,y}, T_{1,z}, \dots, T_{N_{ns},z}) \quad (3)$$

$$\mathbf{V} = (\mathbf{V}_1, \mathbf{\Omega}_1, \mathbf{V}_2, \mathbf{\Omega}_2, \dots, \mathbf{V}_{N_{ns}}, \mathbf{\Omega}_{N_{ns}}) = (V_{1,x}, V_{1,y}, V_{1,z}, \Omega_{1,x}, \Omega_{1,y}, \Omega_{1,z}, \dots, \Omega_{N_{ns},z}) \quad (4)$$

An important aspect to the approach is the mapping between the individual beads and the nanowires. This is achieved by demanding that the beads comprising a particular nanowire move as a rigid body. The body forces and torques on the  $n$ th nanowire are therefore given by:

$$\mathbf{F}^n = \sum_{i=1}^{n_b} \mathbf{f}_n^i \quad (5)$$

$$\mathbf{T}^n = \sum_{i=1}^{n_b} (\mathbf{r}_n^i - \mathbf{R}_i) \times \mathbf{f}_n^i \quad (6)$$

Conversely, the mapping of linear and angular velocities of a particular nanowire into the velocities of its constituent beads is given by:

$$\mathbf{v}_n^i = \mathbf{V}_n + (\mathbf{R}_n - \mathbf{r}_i^n) \times \mathbf{\Omega}_n \quad (7)$$

## 2.2 Optical Interactions

The optical interactions are calculated using the coupled dipole method (CDM).<sup>4,19–21</sup> The system (here a collection of nano-wires) is decomposed into a collection of dipolar cells, each associated with a point polarizability. Each cell is polarized by a linear superposition of the external field and the electric field scattered by every other cell in the simulation. This interaction term is carried by the dipole interaction tensor. A set of coupled linear equations for the polarization of each cell is obtained which can be solved iteratively. Once the polarization on each cell has been acquired, the force on each cell is obtained from the Lorentz force law,<sup>4</sup> in the form:

$$f_i = \frac{1}{2} (p_j \partial_i E_j^*) \quad (8)$$

Equation (8) is a general expression for the  $i$ th component of the force,  $f_i$ , on a small sphere.  $p_j$  is the  $j$ th component of its polarization, and  $E_j$  the  $j$ th component of the electric field. The force and torque on each nanowire is found by summing the forces on the cells using Eqs. (5,6).

## 2.3 Hydrodynamic Interactions

The diffusion matrix for the system of constituent beads is written down to first order using the Oseen tensor or, to next highest order, using the Rotne-Prager tensor. For greater accuracy, more higher-order terms (or *reflections*) may be included.<sup>22</sup> The diffusion matrix for the system of nanowires then needs to be derived. To achieve this, first the bead diffusion matrix is inverted, to give a friction matrix for the system of beads. Next, the individual nanowires are considered as discrete entities and unitary translational and rotational velocities applied to each wire in turn. Using the friction matrix for the system of beads, the force on all beads in the system can be evaluated. These forces are then reduced to the body forces and torques experienced by each wire

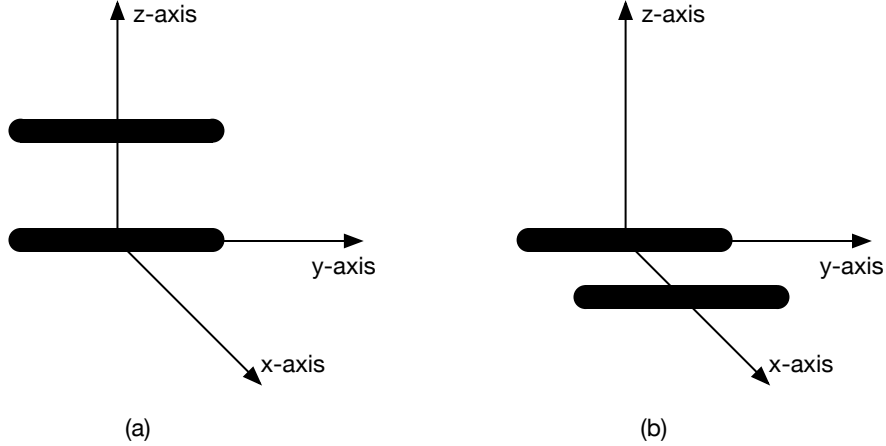


Figure 1. Schematic showing the axes used throughout this paper. The  $x$ -axis corresponds to the direction of the counterpropagating plane waves, and the  $y$ -axis represents the polarisation direction. In (a), the two nanowires form a ladder-like structure, with the rungs of the ladder separated by approximately the wavelength of the incident light field in the  $z$ -direction. Both nanowires are in the same standing-wave maximum of the light field. In (b) the two nanowires are in adjacent bright maxima, half a wavelength apart.

using Eqs. (5,6). Thus, a friction matrix for the system of nanowires is developed, inversion of which yields the diffusion matrix for the nanowire system. This matrix allows dynamical simulations to be performed.

In the case of cylindrically symmetric structures, such as nanowires, the friction matrix for the system of wires becomes singular and cannot be inverted. To overcome this problem, the degree of freedom associated with rotations about the wire axis, needs to be dispensed with prior to inversion.

## 2.4 Brownian Dynamics

The availability of the optical forces experienced by each nanowire, and the acquisition of the diffusion matrix, permits integration of the Langevin equation for the system of nanowires. This has been presented elsewhere, for systems of spheres.<sup>23</sup> However, the derivation is not explicitly restricted to spherical particles and can be extended to arbitrary structures.<sup>24</sup> The resulting displacements of the nanowires are given by:

$$\Delta = \mathbf{D}\mathbf{F}\Delta t + \nabla \cdot \mathbf{D}\Delta t + \mathbf{R}(\Delta t) \quad (9)$$

where,  $\Delta = (\delta\mathbf{r}_1, \delta\theta_1, \delta\mathbf{r}_2, \delta\theta_2, \dots, \delta\theta_{N_{ns}})$  with  $\delta\mathbf{r}_n$  being the displacement of the centre of mass of the  $n$ th wire and  $\delta\theta_n$  a rotation that acts on the orientation of the structure.  $\mathbf{D}$  is the diffusion matrix for the system of nanowires. The total displacement,  $\Delta$  consists of three terms. The first is a displacement resulting from the applied forces  $\mathbf{F}$  and the second is proportional to the divergence of the diffusion matrix. The effect of the divergence term is found to be negligible in the regime in which we are working, and it may be safely ignored.  $\mathbf{R}$  is a vector of translational and rotational displacements drawn from a multivariate normal distribution such that  $\langle \mathbf{R} \otimes \mathbf{R} \rangle = 2k_B T \mathbf{D}$ .

## 2.5 Model Parameters

The simulations consist of a pair of nanowires, arranged as shown in Fig. 1. The nanowires consist of beads of diameter between 50 nm and 100 nm. The lengths of the nanowires range from 0.3  $\mu\text{m}$  to 3.0  $\mu\text{m}$ , and a nominal refractive index of 2.6 is used throughout. The wavelength of the incident counterpropagating waves (incident parallel to the  $\pm x$ -axes) is 800 nm, and the medium is taken as water. The polarisation direction is parallel to the  $y$ -axis. We consider the geometry and stability of pairs of nanowires arranged either as a ladder in the  $z$ -direction (Fig. 1(a)) or stacked in the  $x$ -direction (Fig. 1(b)).

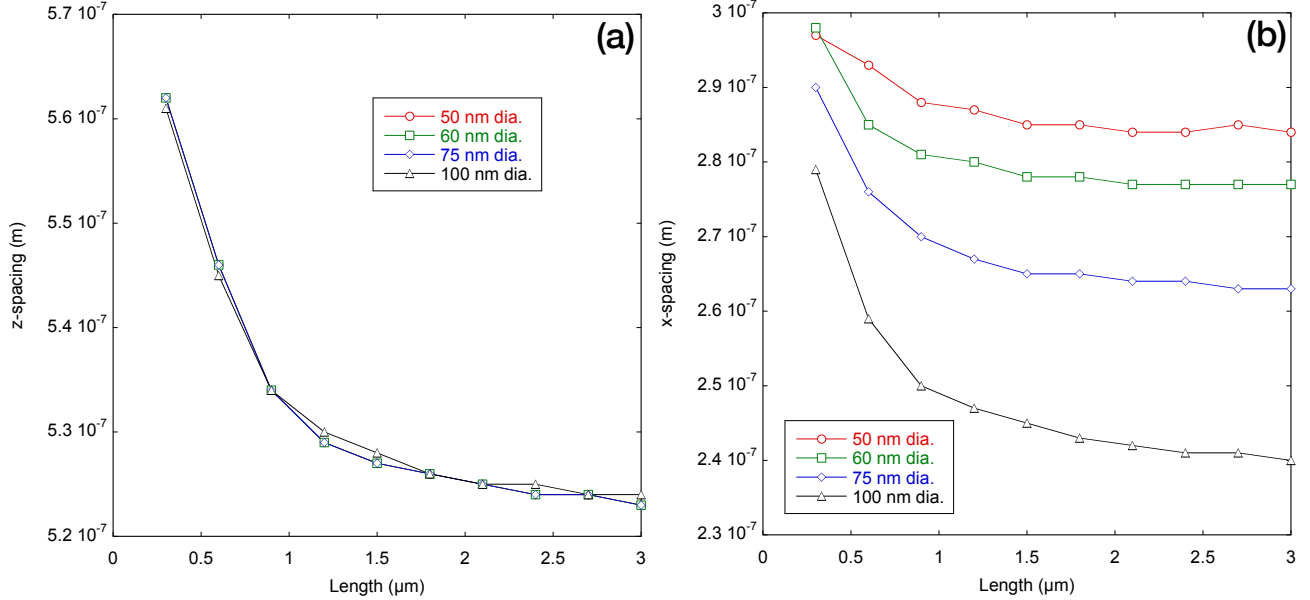


Figure 2. The spacing between two nanowires arranged as in Fig. 1 as a function of nanowire length, for different diameters: (a) the  $z$  separation for two nanowires in the same bright fringe and (b) the  $x$ -separation between two nanowires in adjacent bright fringes.

### 3. RESULTS

#### 3.1 Equilibrium Nanowire Separation

As is well known, the orientation of an extended object in an optical field is sensitive to both the electric polarization and to inhomogeneities in the intensity of an incident optical field. In the present case, this means that the nanowires tend to lie in the bright fringes of the counterpropagating waves, and orient themselves with the polarisation direction ( $y$ -axis). As previously noted,<sup>18</sup> strong optical binding interactions cause the nanowires to form stacks either in the propagation direction ( $x$ -axis), in which case the centres of the wires will correspond to the positions of the bright fringes, or perpendicular to the propagation direction ( $z$ -axis) in which case the separation is nominally a whole number of wavelengths of the incident light in the medium.

The equilibrium separation between such nanowire pairs is examined in Fig. 2, for a range of nanowire lengths and diameters. Figure 2(a) shows the influence of nanowire length on the separation of two nanowires arranged in the  $z$  direction. It is apparent that the separation quickly decreases from the nominal one-wavelength separation (600 nm) for nanowires greater than  $1 \mu\text{m}$  in length, and appears to be reaching a plateau at around 525 nm for longer wires. Interestingly the diameter of the nanowires does not appear to influence the  $z$ -spacing.

It is a different story, however, when the nanowires are arranged in adjacent bright fringes (Fig. 2(b)). The separation of bright fringes is 300 nm, but only the shortest and narrowest nanowires, i.e. those with the weakest binding interactions, come close to this separation. Otherwise, it is found that the increase in length leads to a greater attraction between the wires that is acting against the incident intensity distribution. The effect is substantially greater for the wider nanowires: those of 100 nm diameter have an equilibrium separation of only around 240 nm for wires over  $1 \mu\text{m}$  in length.

#### 3.2 Ladder Stability

We examine the relative stability of nanowire pairs, arranged either one above the other in a single bright fringe (Fig. 1(a)) or side-by-side in adjacent bright fringes (Fig. 1(b)). In each case we examine the thermal motion in the equilibrium configurations that are established. We define an effective stiffness using:

$$K_q^{eff} = \frac{k_B T}{\langle \text{Var}(\Delta q) \rangle}. \quad (10)$$

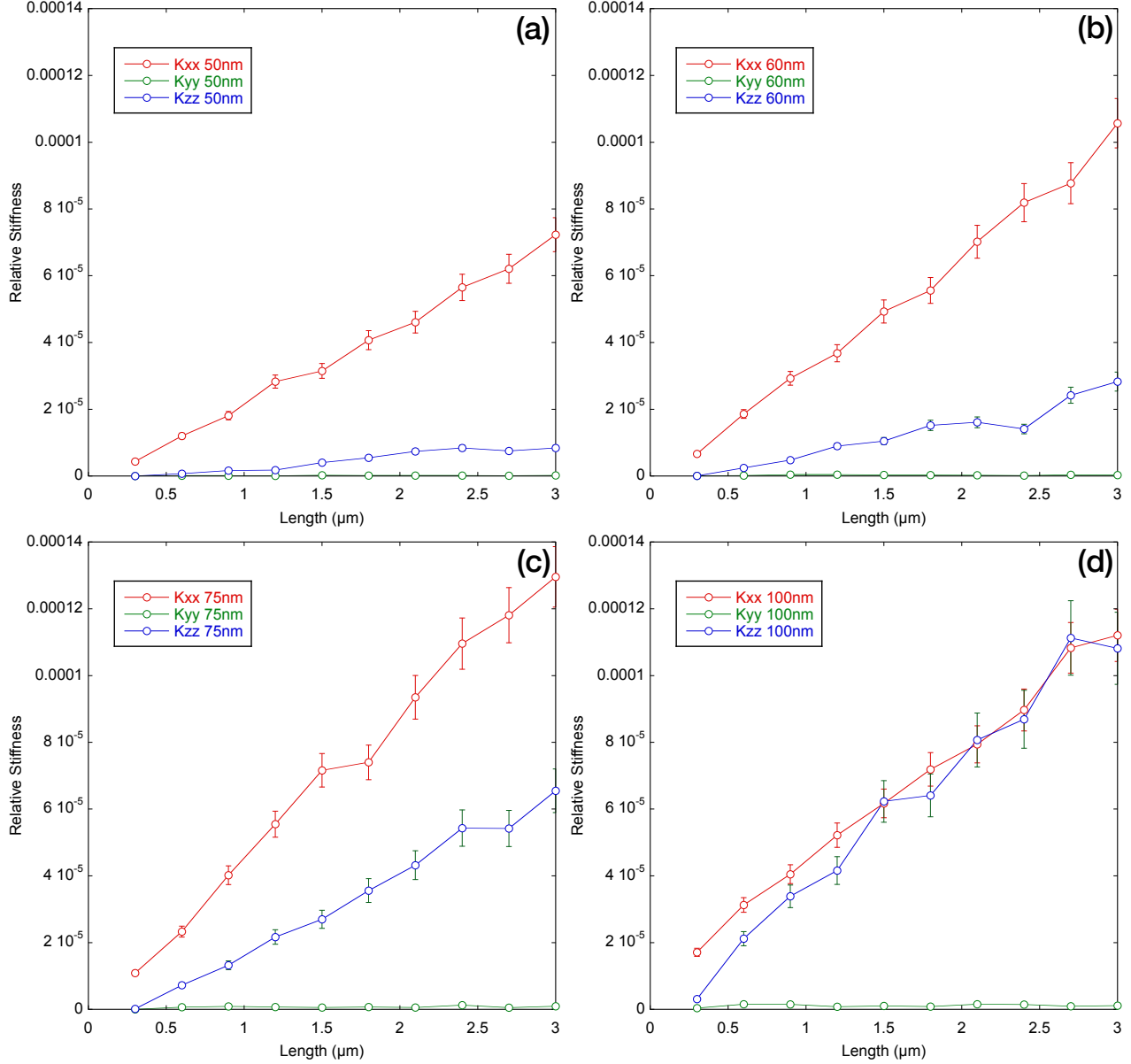


Figure 3. The displacement stiffness acting between two nanowires in a ladder configuration, as a function of nanowire length for diameters of (a) 50 nm, (b) 60 nm, (c) 75 nm and (d) 100 nm.

where  $\langle \text{Var}(\Delta q) \rangle$  is the variance of the difference in  $x$ ,  $y$  or  $z$  coordinates of the nanowires. Low values of stiffness equate to a lack of thermal stability. We do not consider the angular stiffnesses, as these are dominated by the orienting effects of the linear polarisation and the fringe intensity.

Figure 3 shows the effect of nanowire length and diameter on the displacement stiffnesses of two nanowires arranged as a ladder in the  $z$  direction. In all cases  $K_{xx}$  dominates, which indicates the nanowires being confined by the bright fringe intensity.  $K_{zz}$  is a measure of the stability to pulling the nanowires apart along the  $z$  axis. This shows a relatively low value for the 50 nm diameter wires ( $1 \times 10^{-5}$ ) but increases by an order of magnitude when the diameter is doubled to 100 nm. Both  $K_{xx}$  and  $K_{zz}$  increase approximately linearly with the nanowire length. Interestingly,  $K_{yy}$ , which corresponds to a shearing of the nanowires parallel to the polarisation direction, is very low in all cases, indicating that the ladder arrangement is least stable to this type of deformation.

A similar set of graphs for two nanowires, placed in adjacent fringes, is shown in Fig. 4. As with the previous

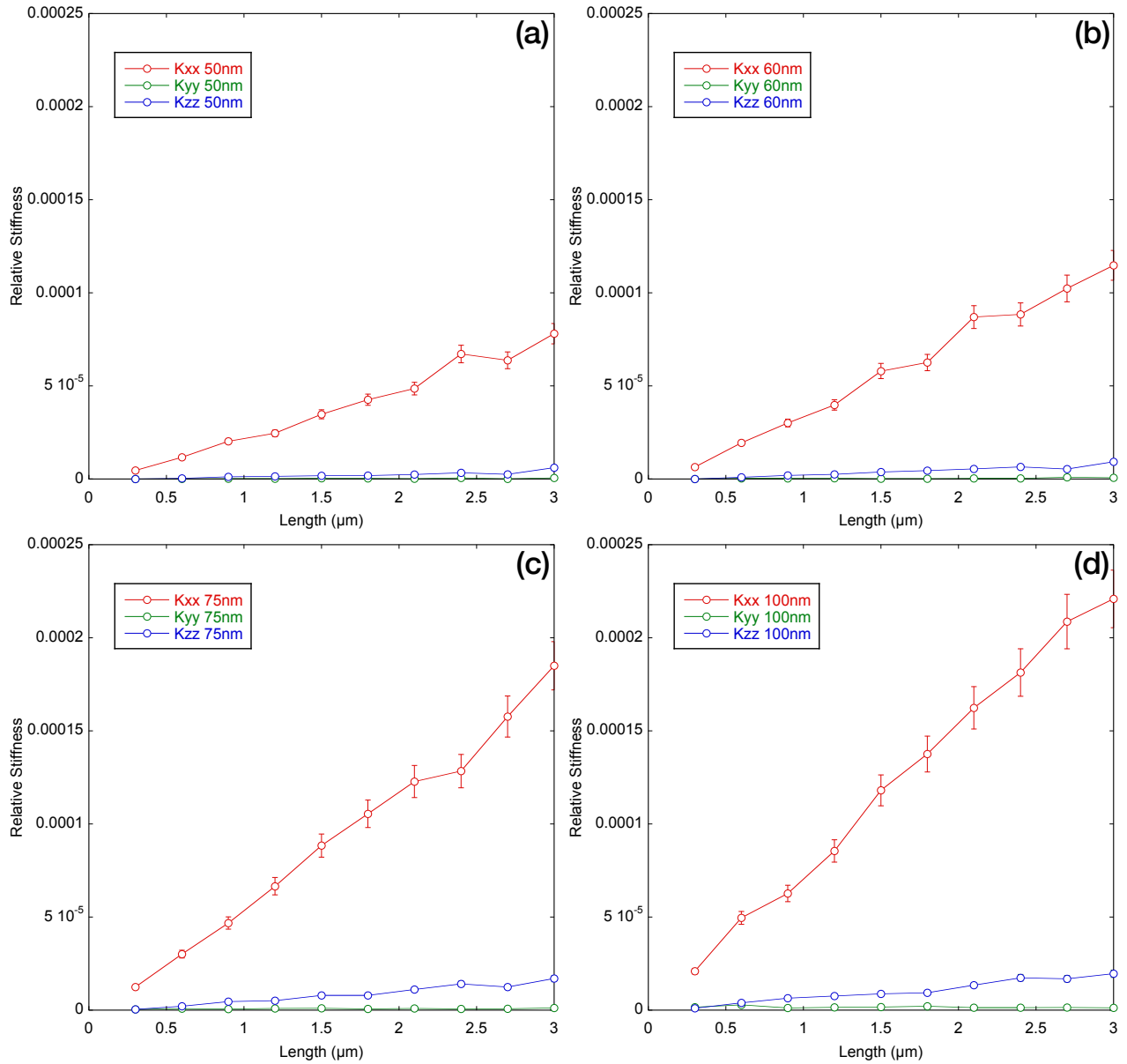


Figure 4. The displacement stiffness acting between two nanowires in adjacent bright fringes, as a function of nanowire length for diameters of (a) 50 nm, (b) 60 nm, (c) 75 nm and (d) 100 nm.

arrangement,  $K_{xx}$  dominates, due to the bright intensity fringes. However, this value now refers to the separation between the nanowires. Interestingly, for the 50 nm nanowires, there appears little difference between  $K_{xx}$  for the two arrangements studied i.e. in both cases, the stiffness has a value of around  $7 \times 10^{-5}$  for the longest wires studied. However, differences occur as the nanowire diameter increases and, for the largest diameter considered (100 nm)  $K_{xx}$  is approximately double in the  $x$  configuration compared with the value found in the  $z$  configuration.

The perpendicular stiffness,  $K_{zz}$  remains comparatively small for all nanowire geometries and, as previously, the shearing stiffness  $K_{yy}$  is the smallest, and appears little influenced by with the nanowire length or diameter.

#### 4. DISCUSSION

We have examined the thermal stability of pairs of nanowires, optically bound in a ladder-like arrangement, in two configurations in counterpropagating beams. As expected, the nanowire pairs assume two equilibrium configurations, as indicated in Fig. 1. In the  $z$  configuration, the nanowires are separated in the  $z$  direction, perpendicular to the propagation direction. The spacing of the nanowires decreases from nominally one wavelength (600 nm) for the shortest wires, to around 85% of this figure for the longest wires examined. The lack of any influence from the nanowire diameter is a little surprising. However, the stiffness  $K_{zz}$  shows a marked increase with diameter—an order of magnitude increase in  $K_{zz}$  for a doubling of nanowire diameter—which shows that while the equilibrium separation is insensitive to diameter, the effective well-depth is not. Other simulation results, not shown here, suggest that the equilibrium separation is sensitive to refractive index, decreasing as the refractive index increases.<sup>25</sup> In this configuration,  $K_{xx}$  relates to displacements relative to the bright fringes.  $K_{xx}$  increases with the diameter of the nanowires, while both  $K_{xx}$  and  $K_{zz}$  increase with their length. The longitudinal stiffness,  $K_{yy}$ , corresponds to shear deformations of the nanowire pair. It takes very small values and is relatively insensitive to the geometry of the particles.

For two nanowires in the  $x$  configuration, the particle separation is expected to be set by the separation of the bright fringes. However, it is found to decrease significantly from this value, especially for the larger (longer and wider) nanoparticles. This has intriguing consequences for the stability of larger stacks of wires in this configuration.<sup>25</sup> The interparticle stiffness,  $K_{xx}$ , is large than the corresponding values for the  $z$  configuration, presumably due to the contribution from the bright fringes. As with the  $z$  configuration, the shear stiffness,  $K_{yy}$  is relatively small, suggesting that the designation of “ladder-like” structure should perhaps be modified to “rope-ladder”.

The model employed has computed the full optical and hydrodynamic interactions, allowing the dynamics to be followed by implementing a Brownian dynamics simulation. The method employed is to represent the nanowires by a set of spheres, which act as the centres of interaction for both the hydrodynamic and optical calculations. The nanowires are minimally represented by a single line of spheres, constrained to move as rigid bodies. Consequently, the nanowire diameters correspond to the sphere diameters employed.

This geometric rendering of the nanowires is quite crude, necessitated, in part, by the computational burden of increasing the number of beads, or cells. The optical computations could be eased using techniques described elsewhere.<sup>4</sup> However, while there is no immediately obvious way of improving the hydrodynamic calculations, the hydrodynamic system does not suffer too badly when the geometric resolution is poor. This is a consequence, in part, of the containment theorems of low Reynolds number hydrodynamics,<sup>26</sup> which prevent coarse grained calculations from becoming wildly inaccurate. A possible route to improved realism may be to use different resolutions; a fine discretization for the optical problem, which could be tackled iteratively as shown in Ref.,<sup>4</sup> and a coarser approach could be employed for the hydrodynamic problem. This is the subject of future efforts.

#### ACKNOWLEDGMENTS

The authors thank ISI Brno for financial support for S.H.S. and the University of Bristol Advanced Computing Research Centre (<http://acrc.bris.ac.uk/>) for provision of computing resources.

## REFERENCES

- [1] Burns, M. M., Fournier, J.-M., and Golovchenko, J. A., “Optical binding,” *Physical Review Letters* **63**(12), 1233 (1989).
- [2] Singer, W., Frick, M., Bernet, S., and Ritsch-Marte, M., “Self-organized array of regularly spaced microbeads in a fiber-optical trap,” *JOSA B* **20**(7), 1568–1574 (2003).
- [3] Taylor, J. and Love, G., “Spontaneous symmetry breaking and circulation by optically bound microparticle chains in gaussian beam traps,” *Physical Review A* **80**(5), 053808 (2009).
- [4] Karásek, V., Brzobohatý, O., and Zemánek, P., “Longitudinal optical binding of several spherical particles studied by the coupled dipole method,” *Journal of Optics A: Pure and Applied Optics* **11**(3), 034009 (2009).
- [5] Metzger, N., Dholakia, K., and Wright, E., “Observation of bistability and hysteresis in optical binding of two dielectric spheres,” *Physical Review Letters* **96**(6), 068102 (2006).
- [6] Čížmár, T., Romero, L. D., Dholakia, K., and Andrews, D., “Multiple optical trapping and binding: new routes to self-assembly,” *Journal of Physics B: Atomic, Molecular and Optical Physics* **43**(10), 102001 (2010).
- [7] Demergis, V. and Florin, E.-L., “Ultrastrong optical binding of metallic nanoparticles,” *Nano Letters* **12**(11), 5756–5760 (2012).
- [8] Yan, Z., Shah, R. A., Chado, G., Gray, S. K., Pelton, M., and Scherer, N. F., “Guiding spatial arrangements of silver nanoparticles by optical binding interactions in shaped light fields,” *ACS Nano* **7**(2), 1790–1802 (2013).
- [9] Nome, R. A., Guffey, M. J., Scherer, N. F., and Gray, S. K., “Plasmonic interactions and optical forces between au bipyramidal nanoparticle dimers,” *The Journal of Physical Chemistry A* **113**(16), 4408–4415 (2009).
- [10] Andrews, D. L. and Bradshaw, D. S., “Laser-induced forces between carbon nanotubes,” *Optics Letters* **30**(7), 783–785 (2005).
- [11] Cölfen, H. and Mann, S., “Higher-order organization by mesoscale self-assembly and transformation of hybrid nanostructures,” *Angewandte Chemie International Edition* **42**(21), 2350–2365 (2003).
- [12] Mann, S., “Self-assembly and transformation of hybrid nano-objects and nanostructures under equilibrium and non-equilibrium conditions,” *Nature Materials* **8**(10), 781–792 (2009).
- [13] Irrera, A., Artoni, P., Saija, R., Gucciardi, P. G., Iatì, M. A., Borghese, F., Denti, P., Iacona, F., Priolo, F., and Maragò, O. M., “Size-scaling in optical trapping of silicon nanowires,” *Nano letters* **11**(11), 4879–4884 (2011).
- [14] Maragó, O. M., Bonaccorso, F., Saija, R., Privitera, G., Gucciardi, P. G., Iatì, M. A., Calogero, G., Jones, P. H., Borghese, F., Denti, P., et al., “Brownian motion of graphene,” *ACS nano* **4**(12), 7515–7523 (2010).
- [15] Ridolfo, A., Saija, R., Savasta, S., Jones, P. H., Iatì, M. A., and Marago, O. M., “Fano-doppler laser cooling of hybrid nanostructures,” *ACS nano* **5**(9), 7354–7361 (2011).
- [16] Wang, F., Toe, W. J., Lee, W. M., McGloin, D., Gao, Q., Tan, H. H., Jagadish, C., and Reece, P. J., “Resolving stable axial trapping points of nanowires in an optical tweezers using photoluminescence mapping,” *Nano letters* **13**(3), 1185–1191 (2013).
- [17] Reece, P. J., Toe, W. J., Wang, F., Paiman, S., Gao, Q., Tan, H. H., and Jagadish, C., “Characterization of semiconductor nanowires using optical tweezers,” *Nano letters* **11**(6), 2375–2381 (2011).
- [18] Simpson, S. H., Jones, P. H., Marago, O. M., Hanna, S., and Miles, M. J., “Optical binding of nanowires in counterpropagating beams,” *Proc. SPIE* **8810**, 881026 (2013).
- [19] Yurkin, M. A., Maltsev, V. P., and Hoekstra, A. G., “The discrete dipole approximation for simulation of light scattering by particles much larger than the wavelength,” *Journal of Quantitative Spectroscopy and Radiative Transfer* **106**(1), 546–557 (2007).
- [20] Simpson, S. H. and Hanna, S., “Application of the discrete dipole approximation to optical trapping calculations of inhomogeneous and anisotropic particles,” *Optics Express* **19**(17), 16526–16541 (2011).
- [21] Simpson, S. H., Phillips, D., Carberry, D., and Hanna, S., “Bespoke optical springs and passive force clamps from shaped dielectric particles,” *Journal of Quantitative Spectroscopy and Radiative Transfer* **126**, 91–98 (2013).



- [22] Happel, J. and Brenner, H., [*Low Reynolds number hydrodynamics: with special applications to particulate media*], vol. 1, Springer (1965).
- [23] Ermak, D. L. and McCammon, J., “Brownian dynamics with hydrodynamic interactions,” *The Journal of chemical physics* **69**, 1352 (1978).
- [24] Brady, J. F. and Bossis, G., “Stokesian dynamics,” *Annual Review of Fluid Mechanics* **20**, 111–157 (1988).
- [25] Simpson, S. H. and Hanna, S., “Paper in preparation,” (2016).
- [26] Kim, S. and Karrila, S. J., [*Microhydrodynamics: principles and selected applications*], DoverPublications.com (1991).